

## CRITICAL PHENOMENA IN PARTICLE DISSOLUTION IN THE MELT DURING ELECTRON-BEAM SURFACING

O. N. Kryukova and A. G. Knyazeva

UDC 536.46+621.9

*A model for the electron-beam surfacing process is proposed that takes into account the dissolution of the modifying particles in the melt. Critical conditions are determined for various modes of surfacing resulting in nearly homogeneous or composite coatings. A detailed parametric study of the one-dimensional version of the model is performed.*

**Key words:** *surfacing, dissolution, critical conditions, thermal conductivity.*

**Introduction.** Recent progress in surfacing and coating technologies has stimulated the mathematical modeling of the processes determining the properties of the materials produced. High-temperature technologies of this type are based on the use of chemical energy sources or include various physical and chemical processes similar to those traditionally studied in combustion theory. This, in particular, is characteristic of electron-beam processing of materials. The well-known models of electron-beam processing take into account only thermal processes (heating, melting, crystallization) or analyze only hydrodynamic flow in the molten pool. There is a variety of electron-beam surface coating technologies. In some of them, the material surface is first coated with a powder layer and the material with the coating is then subjected to thermal treatment with an electron beam [1]. In other technologies, a coating is formed directly during thermal treatment by interaction of the particles fed into the melt with the base material [2–5]. The phase and chemical structures of the resulting coating depend greatly on the chemical composition of the treated material, the powder used to modify the properties, and process parameters. In addition, the physical and chemical processes determining the properties of the materials produced and the physical and mathematical models used to treat and describe the observed regularities [6–10] are also different.

The real powders used to modify the surfaces of materials in order to improve their strength properties, have complex compositions; their interaction with the base melt formed behind the moving scanning electron beam (in practice [2], the part being treated moves) is accompanied by various physical and chemical transformations, which cannot be described using one model without preliminary studies. Therefore, theoretical studies have been performed using special modeling systems, each of which is characterized by a particular type of interaction of the molten base and modifying particles. There are two types of modifying particles: insoluble and soluble. The first are characterized by different wettability of the molten base and, as a consequence, by different coupling with the solid matrix. This ultimately influences the mechanical properties of the coatings. Modifying particles [4, 5], but is of no significance for the electron-beam surfacing technology. An example of a system with insoluble particles is the W–Cu system. The one-dimensional mathematical model formulated and investigated in detail in [6, 9] for this case allows one to determine the relationship between the fraction of particles in the coating formed and the process parameters. From these calculations and using simple formulas available in the literature describing the mechanical properties of composite materials, it is possible to obtain the dependences of the elastic modulus of a coating on the electron beam power density, the beam velocity, and the particle supply rate that are consistent with the observed regularities for real composite powders. The particle size distribution is also important for the

---

Institute of the Physics of Strength and Materials Science, Siberian Division, Russian Academy of Sciences, Tomsk 634021; anna@ispms.tsc.ru. Translated from *Prikladnaya Mekhanika i Tekhnicheskaya Fizika*, Vol. 48, No. 1, pp. 131–142, January–February, 2007. Original article submitted September 22, 2004; revision submitted February 7, 2006.

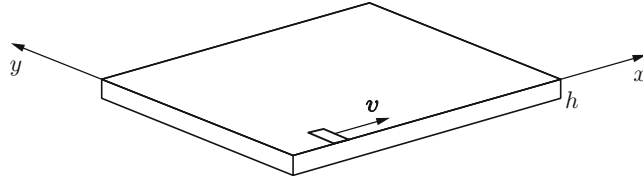


Fig. 1. Motion of the source over the plate surface.

estimation of mechanical properties. However, in the case of soluble particles, it can be assumed that the particle size distribution in the modified surface layer is the same as in the starting powder.

In the second case, i.e., in the case of particles capable of being dissolved in the base material, the mathematical models become complicated. In systems with unlimited mutual solubility, the dissolution of particles of a material in another molten material is determined by diffusion. In this case, the difficulties arising in the description of dissolution based on known representations [11, 12] are due only to the necessity of determining the dissolution constant. A method for estimating the dissolution constant based on experimental data is proposed in [13, 14].

A two-dimensional model of electron-beam surfacing for the Ni–Cu system was studied in detail in [7–9]. Among the results obtained is a nonlinear dependence of the elastic modulus on the process parameters, which is typical of soluble particles.

If dissolution is accompanied by chemical transformations, the system of equations from [7] is supplemented by chemical kinetics equations [10]. An example is the Al–Cu system. Calculations yield the phase and chemical composition of the coating in a quasisteady state, including the fraction of undissolved particles and the concentrations of pure elements and phases.

An analysis of the studies performed shows that among the numerous physical and chemical processes in question, one can distinguish the processes common for different compositions: the formation of a molten pool behind the moving effective source of heat; the redistribution of particles in the melt with a change in the effective heat capacity; additional heat release or absorption due to dissolution by a particular mechanism; heat losses due to radiation. Investigation of an appropriate general model is of interest in the analysis of various conditions of coating formation. Subsequently, this model can be used to optimize the production process. The purpose of the present work is to formulate such a general model and perform a detailed parametric analysis of its one-dimensional version.

**1. Mathematical Formulation of the Problem.** Let a source move over the surface of a plate of thickness  $h$  (Fig. 1). The energy distribution in the source is given by

$$q_e = \begin{cases} 0, & |y| > y_0/2, \\ q_0 \exp(-(x - vt)^2/a_t^2), & |y| \leq y_0/2. \end{cases} \quad (1)$$

Here  $q_0$  is the maximum flux power density,  $a_t$  is the effective radius of the source, the quantity  $y_0$  is proportional to the scanning width, and  $v$  is the velocity of motion of the source along the  $x$  axis. This energy distribution in the source corresponds to sawtooth electron-beam oscillations [15].

At a certain distance  $x_a$  from the energy release maximum (or at the maximum point), particles with properties different from the properties of the material being treated are supplied to the molten pool.

The particle flux density follows a Gaussian distribution

$$q_{\max} = q_{\max,0} \exp[-((x - x_a - vt)^2 + y^2)/a_p^2], \quad (2)$$

where  $q_{\max,0}$  is the maximum particle flux density and the quantity  $a_p$  is defined by the radius of the tube through which the particles are supplied. In some coating technologies, the particles supplied to the melt can be distributed similarly to the energy in the effective source [see (1)].

The temperature distribution is determined by solving the system of the thermal-conductivity equations (with the effective thermal-physical properties) and the kinetic equation for the volume fraction of undissolved particles.

In the laboratory system of coordinates, the thermal-conductivity equation are written as

$$c_{\text{eff}} \rho_{\text{eff}} \left( \frac{\partial T}{\partial t} \right) = \frac{\partial}{\partial x} \left( \lambda_{\text{eff}} \frac{\partial T}{\partial x} \right) + \frac{\partial}{\partial y} \left( \lambda_{\text{eff}} \frac{\partial T}{\partial y} \right) + Q_s \varphi - \frac{\varepsilon \sigma T^4 - q_e}{h},$$

where  $T$  is the temperature, the term  $\varepsilon\sigma T^4$  describes the radiative heat transfer from the plate surface under the Stefan–Boltzmann law,  $c_{\text{eff}}$  is the heat capacity,  $\rho_{\text{eff}}$  is the density,  $\lambda_{\text{eff}}$  is the thermal conductivity,  $Q_s$  is the heat of particle dissolution in the melt, and  $\varphi$  is the kinetic function of dissolution. Generally, thermal-physical characteristics depend on temperature and composition, which is taken into account in descriptions of the electron-beam surfacing of particular systems [4–6]. For a qualitative study of the coating formation process, the thermal conductivity is considered constant ( $\lambda_{\text{eff}} = \text{const}$ ) since, according to literature data, the value of  $\lambda_{\text{eff}}$  depends weakly on the particle volume fraction; in this case, we take into account that the particles supplied to the system change the effective heat capacity of the system:

$$(c\rho)_{\text{eff}} = c\rho(1 - \eta_p) + c_1\rho_1\eta_p,$$

where  $c$  and  $\rho$  are the heat capacity and density of the pure substance of the base or the solution of the particle material in the base and  $c_1$  and  $\rho_1$  are the heat capacity and density of the solid undissolved particles.

In multicomponent systems, melting and crystallization can be described using the theory of a two-phase zone or its modifications (see, for example, [4, 5]). For a qualitative study of the laws of thermal physics, we employ a simpler approach based on thermodynamic reactions. We assume that in the vicinity of the melting point of the base  $T_{\text{ph}}$ , the heat capacity increases sharply:

$$c\rho = \rho_s L_{\text{ph}} \delta(T - T_{\text{ph}}) + (c\rho)_s, \quad T < T_{\text{ph}}, \quad c\rho = \rho_s L_{\text{ph}} \delta(T - T_{\text{ph}}) + (c\rho)_{\text{liq}}, \quad T \geq T_{\text{ph}}.$$

Here the subscript “s” corresponds to the solid phase and the subscript “liq” to the liquid phase;  $\delta$  is the Dirac delta-function ( $\delta \rightarrow \infty$  at  $T = T_{\text{ph}}$  and  $\delta = 0$  for  $T \neq T_{\text{ph}}$ ). In real calculations, the Dirac function is replaced by a delta-shaped function that satisfies the normalization condition  $\int_{-\infty}^{+\infty} \Phi(x) dx = 1$ . This condition is satisfied, for example, for the function [16]

$$\Phi = \frac{1}{\sigma_0 \sqrt{\pi}} \exp \left[ - \left( \frac{T - T_{\text{ph}}}{\sigma_0} \right)^2 \right].$$

The fraction of particles in the melt and the solid phase formed during crystallization can vary widely, and, hence, the known models of suspensions and composite materials are inappropriate for describing particle motion and dissolution in the melt and solid solution formation. In the thermal-physical model, the fraction of particles in the melt (or undissolved inclusions in the solid solution) is determined from the equation

$$\frac{\partial \eta_p}{\partial t} = q_{\text{max}} - \varphi(T, \eta_p, \dots).$$

The function  $\varphi$  describing the dissolution rate generally depends on the temperature, particle size, the mutual solubility of elements, and the local flow characteristics in the melt. According to the theoretical representations of [11, 12], the function  $\varphi(T, \eta_p)$  can be written as

$$\varphi(T, \eta_p) = \varphi_1(\eta_p) k_0 \exp(-E_a/(RT)),$$

which reflects the main regularities of the dissolution process.

If the dissolution rate of solid particles in the melt is determined by diffusion, the value of  $E_a$  is close to the activation energy of diffusion. If the transport of elements from the solid to the liquid phase is accompanied by chemical interaction of elements, then  $E_a$  is a certain effective quantity that depends on the degree of influence of various processes. The form of the kinetic function  $\varphi_1(\eta_p)$  depends on the processes determining the dissolution rate at the microlevel. According to known dissolution models, the constant  $k_0$  is determined by the local characteristics of the hydrodynamic flow. It can be estimated using the well-known theories [11, 12]. The constant  $k_0$  can be determined by processing experimental data in accordance with the model representations of [13, 14]. Generally, the dissolution process can be both endothermic ( $Q_s < 0$ ) and exothermic ( $Q_s > 0$ ), depending on the physical and chemical processes determining the dissolution mechanism.

The condition  $\partial T/\partial y = 0$  at  $y = 0$  is a consequence of symmetry; the conditions  $\partial T/\partial x = 0$  for  $x = 0$  and  $\infty$  and  $\partial T/\partial y = 0$  for  $y \rightarrow \infty$  imply the absence of heat sources and sinks at infinity from the heated region and at the free end of the plate.

At the initial time, we have

$$t = 0: \quad T = T_0, \quad \eta_p = 0,$$

where  $T_0$  is the initial temperature.

**2. Formulation of the Problem in Dimensionless Variables.** We convert to the dimensionless variables

$$\tau = \frac{t}{t_*}, \quad \xi = \frac{x}{x_*}, \quad \eta = \frac{y}{x_*}, \quad \theta = \frac{T - T_0}{T_* - T_0}.$$

Here  $x_* = a_t$ ,  $t_* = a_t/v$  is the time for which the external source travels the distance  $a_t$ , and  $T_* = T_0 + q_0 t_* / (c_s \rho_s h)$  is the characteristic temperature to which a plate of thickness  $h$  is heated for the time  $t_*$ . Then, the mathematical formulation of the problem becomes

$$f_1 \frac{\partial \theta}{\partial \tau} = \frac{1}{\delta} \left( \frac{\partial^2 \theta}{\partial \xi^2} + \frac{\partial^2 \theta}{\partial \eta^2} \right) + S_r \bar{\varphi}(\eta_p, \theta) - (\gamma \theta + 1)^4 B + f_2; \quad (3)$$

$$\frac{\partial \eta_p}{\partial \tau} = f_3 - \bar{\varphi}(\eta_p, \theta); \quad (4)$$

$$\xi \rightarrow 0, \infty: \quad \frac{\partial \theta}{\partial \xi} = 0, \quad \eta \rightarrow 0, \infty: \quad \frac{\partial \theta}{\partial \eta} = 0; \quad (5)$$

$$\tau = 0: \quad \theta = 0, \quad \eta_p = 0, \quad (6)$$

where

$$f_1 = \begin{cases} \frac{S_{\text{ph}}}{\bar{\sigma}_0 \sqrt{\pi}} \exp \left[ - \left( \frac{\theta - \theta_{\text{ph}}}{\bar{\sigma}_0} \right)^2 \right] + (1 - \eta_p) + \eta_p K_s, & \theta < \theta_{\text{ph}}, \\ \frac{S_{\text{ph}}}{\bar{\sigma}_0 \sqrt{\pi}} \exp \left[ - \left( \frac{\theta - \theta_{\text{ph}}}{\bar{\sigma}_0} \right)^2 \right] + (1 - \eta_p) K_{\text{liq}} + \eta_p K_s, & \theta \geq \theta_{\text{ph}}; \end{cases}$$

$$f_2 = \begin{cases} 0, & \eta > \eta_0, \\ \exp(-(\xi - \tau)^2), & |\eta| \leq \eta_0; \end{cases}$$

$$f_3 = \eta_{\text{max}} \exp[-((\xi - \tau)^2 + \eta^2)/r_p^2];$$

$$\bar{\varphi}(\eta_p, \theta) = \varphi_1(\eta_p) \varphi_2(\theta);$$

$$\varphi_1(\eta_p) = \eta_p; \quad \varphi_2(\theta) = \tau_r \exp[-(\gamma + 1)/(\beta(1 + \gamma\theta))];$$

$\delta = a_t^2 / (\varkappa_T t_*)$  is the Frank-Kamenetskii parameter,  $\tau_r = t_* k_0$  is the dimensionless dissolution constant,  $S_r = Q_s / (c_s \rho_s (T_* - T_0))$  is the ratio of the heat of dissolution to the amount of heat in the heated layer,  $B = (1/h) \varepsilon \sigma (T_* - T_0)^3 t_* / (c_s \rho_s \gamma^4)$  is a dimensionless parameter that describes heat losses,  $\beta = RT_* / E_a$  is the ratio of the temperature due to external heating to the activation temperature of the dissolution process  $E_a / R$ ,  $S_{\text{ph}} = L_{\text{ph}} / (c_s (T_* - T_0))$  is the ratio of the heat of melting to the amount of heat in the heated layer,  $\gamma = (T_* - T_0) / T_0$ ,  $K_{\text{liq}} = c_{\text{liq}} \rho_{\text{liq}} / (c_s \rho_s)$ ,  $K_s = c_p \rho_p / (c_s \rho_s)$ ,  $\theta_{\text{ph}} = (T_{\text{ph}} - T_0) / (T_* - T_0)$ ,  $\bar{\sigma}_0 = \sigma_0 / (T_* - T_0)$ ,  $\eta_{\text{max}} = q_{\text{max},0} t_*$ ,  $r_p = a_p / a_t$ ,  $\eta_0 = h_0 / a_t$ , and  $\varkappa_T = \lambda_s / (c_s \rho_s)$ .

The parameter  $\gamma$  can be expressed in terms of  $\beta$  and the well-known parameter of combustion theory — the Zel'dovich number  $Z = (T_* - T_0) E_a / (RT_*^2)$ :

$$\gamma = \frac{T_* - T_0}{T_0 - T_* + T_*} = \frac{1}{(T_* / (T_* - T_0)) - 1} = \frac{Z\beta}{1 - Z\beta}.$$

A detailed study of the two-dimensional problem is time-consuming, which is not always justified. If in (1)  $y_0 \gg a_t$  or, in the dimensionless formulation,  $\eta_0 \gg 1$  and the particle distribution follows the same law as the energy supplied, one can pass to a one-dimensional formulation of the problem, whose analysis provides many qualitative regularities of the two-dimensional model. In this case, the thermal-conductivity equation (3) becomes

$$f_1 \left( \frac{\partial \theta}{\partial \tau} \right) = \frac{1}{\delta} \left( \frac{\partial^2 \theta}{\partial \xi^2} \right) + S_r \bar{\varphi}(\eta_p, \theta) - (\gamma \theta + 1)^4 B + f_2, \quad (7)$$

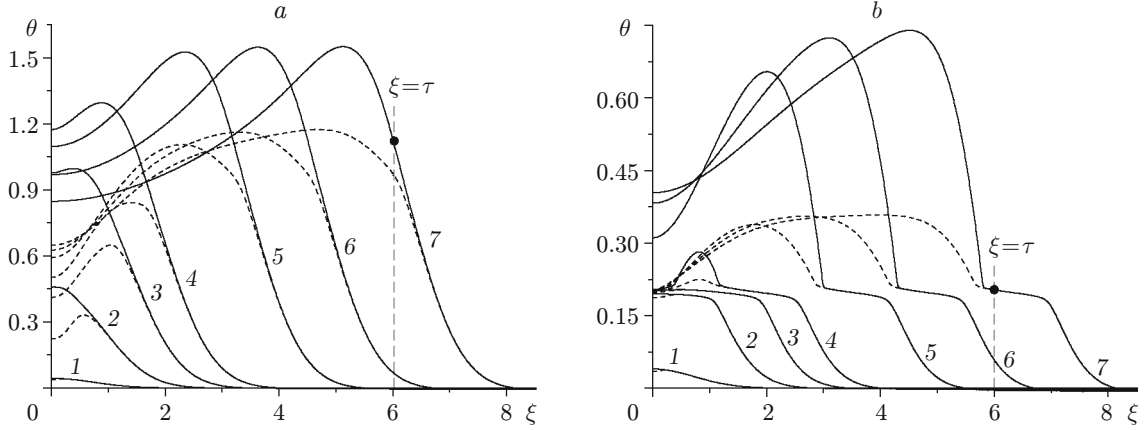


Fig. 2. Temperature distribution along the  $\xi$  axis ignoring particle dissolution ( $\theta_{\text{ph}} = 0.2$ ,  $\gamma = 2$ ,  $\beta = 0.05$ ,  $S_r = 0$ , and  $B = 0.0015$ ) at  $\tau = 0.04$  (1), 0.4 (2), 1 (3), 1.6 (4), 3.2 (5), 4.5 (6), and 6 (7): (a) temperature distribution ignoring the melting of the base ( $S_{\text{ph}} = 0$ ); (b) temperature distribution taking into account melting ( $S_{\text{ph}} = 1$ ); the solid and dashed curves refer to  $K_s = 0.1$  and 10, respectively.

and the form of the kinetic equation (4) does not change. For the functions describing the energy distribution (1) and the fraction of particles (2), we have

$$f_2 = \exp(-(\xi - \tau)^2), \quad f_3 = \eta_{\text{max}} \exp[-(\xi - \tau)^2/r_p^2]. \quad (8)$$

On the surface  $\xi = 0$  and at infinity from this coordinate, heat sources and sinks are absent:  $\partial\theta/\partial\xi = 0$ , and at the initial time, condition (6) is valid.

Using known data on the properties of various substances (Ni, Cu, W, Al, and Cr) [17, 18] and varying the source parameters  $q_0$ ,  $v$ , and  $q_{\text{max},0}$ , we determine the ranges in which the dimensionless parameters vary:  $B = 0-0.1$ ,  $\eta_{\text{max}} = 0.005-3$ ,  $S_r = (-2)-(+2)$ ,  $r_p = 0.1-1.0$ ,  $\tau_r = 10-10^5$ ,  $\beta = 0.01-1.00$ ,  $\gamma = 1-30$ ,  $S_{\text{ph}} = 0.1-10.0$ ,  $\theta_{\text{ph}} = 0.1-36.0$ ,  $K_s = 0.1-10.0$ ,  $K_{\text{liq}} = 0.1-10.0$ , and  $\delta = 0.05-7.00$ .

**3. Analysis of Results of Numerical Study of the One-Dimensional Model.** Problem (4), (6), (7) with conditions (5) for  $\xi$  and functions (8) was solved numerically using an absolutely stable implicit difference scheme and a marching method. A similar method for solving difference equations and a similar splitting scheme were used for the two-dimensional problem. The quantity  $\bar{\sigma}_0$  was chosen so as to provide the most accurate description of the temperature behavior in the vicinity of the melting point: in the region of a sharp change in the heat capacity  $f_1(\theta)$  in the vicinity of  $\theta_{\text{ph}}$  there was not less than 10–20 points; this was achieved by reducing the time step and the smoothing half-interval. For  $\bar{\sigma}_0 < 0.1$ , the result did not change. In the calculations, the following dimensionless parameters describing particle dissolution in the molten pool were varied:  $\gamma$ ,  $K_s$ ,  $\tau_r$ ,  $S_{\text{ph}}$ ,  $\beta$ ,  $\theta_{\text{ph}}$ ,  $B$ , and  $S_r$ . The remaining parameters were fixed:  $\eta_{\text{max}} = 1.5$ ,  $r_p = 0.1$ , and  $\delta = 5$ .

Below we give some results of the numerical study of the electron-beam surfacing process using the model proposed. An analysis of the numerical calculation results shows that, as in fuller models [6–10], the process reaches a quasisteady state in a certain time interval from the beginning of motion of the source. In the absence of particle dissolution, this implies that the maximum temperature (Fig. 2) and the maximum volume fraction of the particles gradually filling the region behind the moving source (not shown in Fig. 2) become constant.

If melting is ignored (Fig. 2a), curves  $\theta(\xi)$  are fairly smooth. The maximum temperature does not correspond to the point  $\xi = \tau$ , at which the energy release from the external source is maximal, and this agrees with the well-known data [15]. The higher the heat capacity  $K_s$  of the particles entering the system, in comparison with the heat capacity of the base, the lower the temperature in the heated region, which is obviously due to the heat losses due to particle heating (dashed curves in Fig. 2a).

Accounting for the melting of the base (Fig. 2b) results in the appearance of a characteristic plateau on the curves of  $\theta(\xi)$ , which is caused by heat absorption as a result of melting. Accounting for melting leads to a decrease in the maximum temperature and an increase in the temperature difference due to the different heat capacities

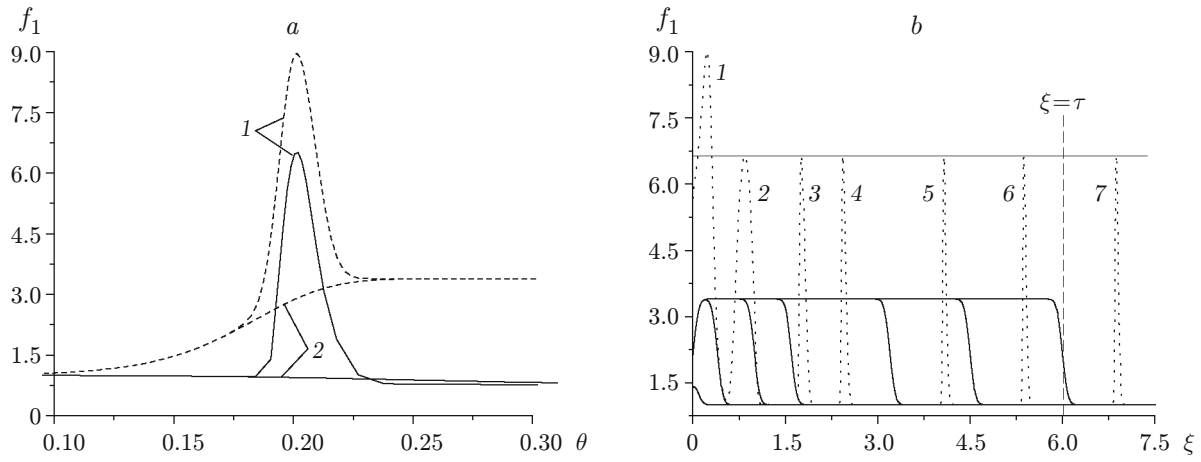


Fig. 3. Effective heat capacity versus temperature at the point  $\xi = 0.25$  (a) and the coordinate (b) for  $\beta = 0.05$ ,  $S_r = 0$ ,  $\tau_r = 0$ ,  $\gamma = 2$ ,  $\theta_{ph} = 0.2$ , and  $B = 0.0015$ : (a) effective heat capacity taking into account the melting of the base (curves 1) and ignoring melting (curves 2) for  $K_s = 0.1$  (solid curves) and 10 (dashed curves); (b)  $K_s = 10$ ,  $S_{ph} = 0$  (solid curves) and 0.1 (dotted curves), and  $\tau = 0.04$  (1), 0.4 (2), 1 (3), 1.6 (4), 3.2 (5), 4.5 (6), and 6 (7); the steady state is shown by a thin solid line.

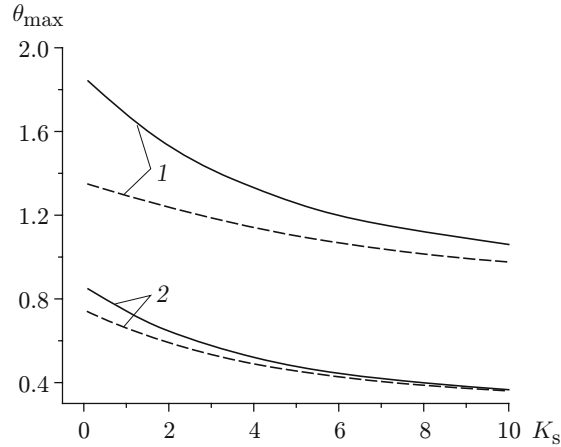


Fig. 4. Maximum temperature versus heat capacity of the particles for  $B = 0$  (solid curves), and 0.0015 (dashed curves) and  $S_{ph} = 0.1$  (1) and 1 (2);  $S_r = 0$ ,  $\tau_r = 0$ , and  $\gamma = 2$ .

of the particles. The maximum of  $\theta_{max}$  moves farther away from the point  $\xi = \tau$ . It is obvious that the higher the heat of the phase transition  $S_{ph}$ , the more pronounced the plateau in the curves of  $\theta(\xi)$  and the smaller the value of  $\theta_{max}$ , which is due to the temperature dependence of the heat capacity (Fig. 3a): in the vicinity of the phase transition temperature, the quantity  $f_1$  increases sharply, resulting in an increase in the heat losses due to the heating of the system.

The variation in the effective heat capacity during motion of the molten pool behind the moving source is shown in Fig. 3b.

If the heat of melting is ignored, then the effective heat capacity varies from unity to  $f_{1,s} = [K_s \eta_p + 1 - \eta_p]$  because of the supply of particles. If the melting of the base is taken into account, the heat capacity  $f_1$  increases sharply at the temperature  $\theta_{ph}$  and then approaches  $f_{1,s}$  again as a result of particle supply.

In the case of insoluble particles, the maximum temperature of the melt in the steady state of the surfacing process obviously decreases with increase in the heat capacity of the particles  $K_s$ , the heat of the phase transition  $S_{ph}$ , and the heat release parameter  $B$  (Fig. 4).

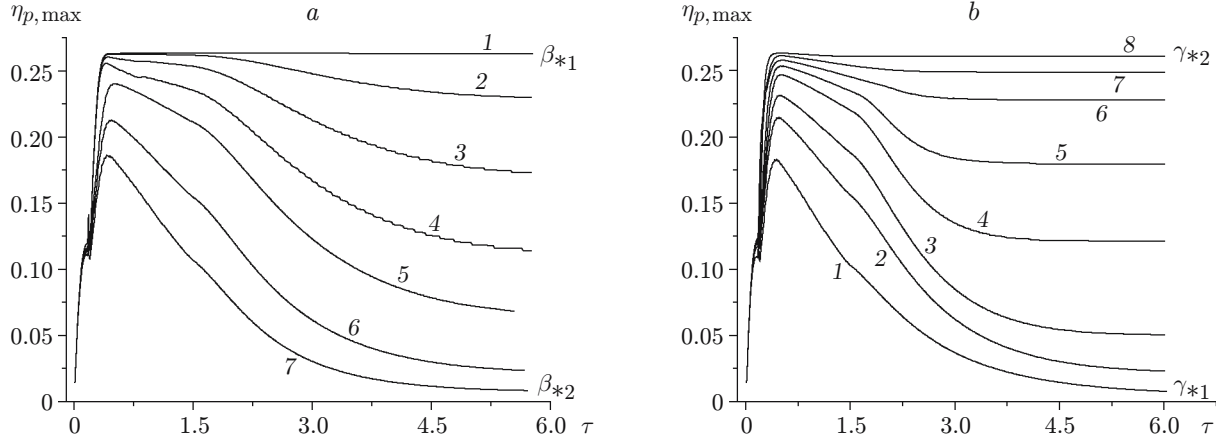


Fig. 5. Maximum volume fraction of particles versus time ( $S_{ph} = 1$ ,  $K_s = 0.1$ ,  $B = 0.0015$ ,  $S_r = 0$ ,  $\delta = 5$ ,  $\tau_r = 10$ ): (a)  $\gamma = 2$  and  $\beta = 0.16$  (1), 0.3 (2), 0.4 (3), 0.5 (4), 0.6 (5), 0.8 (6), and 1 (7); (b)  $\beta = 0.8$  and  $\gamma = 1$  (1), 2 (2), 3 (3), 5 (4), 7 (5), 10 (6), 15 (7), and 20 (8).

If the heat release is ignored, then in the case of insoluble particles, the parameter  $\gamma$  does not influence the calculation results. We note that if the heat release is taken into account, the quasisteady state is established faster and the maximum temperature decreases and depends greatly on the parameter  $\gamma$ . For example, for  $K_s = 1$ ,  $S_{ph} = 0$ ,  $\beta = 0.05$ ,  $\tau_r = 0$ , and  $B = 0$ , we have  $\theta_{max} = 1.75$  for  $\gamma = 2$  and 10; for  $B = 10^{-5}$ , we have  $\theta_{max} = 1.35$  and 0.40 at  $\gamma = 2$  and 10, respectively; for  $B = 0.0015$ , we have  $\theta_{max} = 1.74$  and 1.28 for  $\gamma = 2$  and 10, respectively. The temperature distribution does not change qualitatively.

If particle dissolution is taken into account, the maximum temperature depends on the parameters describing this process: for  $S_r < 0$ , the maximum temperature decreases in comparison with the case  $S_r = 0$ ; for  $S_r > 0$ , the value of  $\theta_{max}$  increases. In this case, critical phenomena are observed in the model. As the time of establishment, we use the time after which the maximum temperature of the melt and the fraction of undissolved particles (in the case of their partial dissolution) do not change with the specified accuracy. If the particles are dissolved completely, the condition of the establishment of a quasisteady state remains the former. For fixed parameters of the problem, there is a value  $\beta = \beta_{*1}$  that separates the surfacing modes with and without particle dissolution (Fig. 5a).

In the region  $\beta_{*1} < \beta < \beta_{*2}$ , the particles are not completely dissolved and surfacing results in a composite coating with a variable fraction of undissolved particles. The particles percolate into the solution of the base material. For  $\beta < \beta_{*1}$ , a composite coating consisting of particles and a matrix of the starting substance is formed. For  $\beta > \beta_{*2}$ , a homogeneous coating is formed. It should be noted that the critical phenomena are also observed when the remaining parameters are varied (Fig. 5b).

We define  $\beta_{*1}$  as a value of  $\beta$  that, by the moment of reaching the quantity  $\eta_{p,max}$ , differs from the maximum fraction of particles ignoring dissolution by not more than 3–5%. The dependence of the thus defined critical value of  $\beta_{*1}$  on the heat capacity of the particles  $K_s$  for various values of the model parameters is given in Fig. 6.

It is obvious that the larger the value of the dissolution constant  $\tau_r$ , the faster the particle dissolution and the smaller the critical value of  $\beta_{*1}$  that separates the different surfacing modes. The effects of the heat and temperature of the phase transition is ambiguous. For a low heat capacity of the particles ( $K_s < 1$ ), the value of  $\beta_{*1}$  increases with increasing phase transition temperature, and at a high heat capacity of the particles ( $K_s \gg 1$ ), it decreases. This is explained by the mutual effect of various thermal-physical processes: melting, dissolution, heat release, heat conduction.

In addition, the critical conditions of particle dissolution depend on the parameters describing the production process ( $\eta_{max}$ ,  $r_p$ ,  $\delta$ , and  $B$ ), the site of particle supply to the melt, and the parameter describing heat losses.

It should be noted that in the case of exothermic particle dissolution, the formation of a coating by electron-beam surfacing can be characterized by terms known from ignition and combustion theory: the ignition time (the time of the beginning of dissolution), the time of reaching a quasisteady state, combustion temperature (the temperature in the steady state), etc. Moreover, the time dependences of the maximum temperature (Fig. 7a) or the

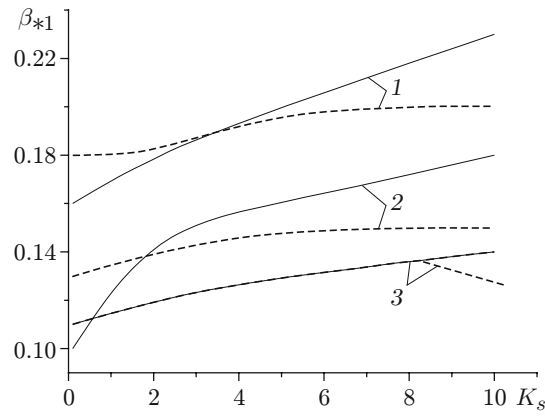


Fig. 6. Critical value of  $\beta_{*1}$  versus heat capacity of particles  $K_s$  for  $\theta_{ph} = 0.2$  (solid curves) and 0.4 (dashed curves): 1)  $\tau_r = 10$  and  $S_{ph} = 1$ ; 2)  $\tau_r = 100$  and  $S_{ph} = 1$ ; 3)  $\tau_r = 10$  and  $S_{ph} = 0.1$ .

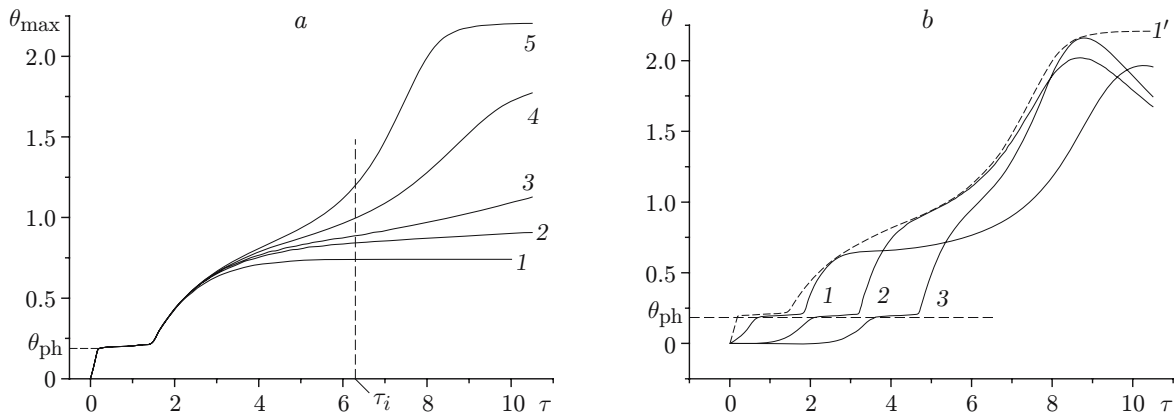


Fig. 7. Maximum temperature (a) and temperatures at various points (b) versus time for various values of the heat of dissolution ( $\beta = 0.2$ ,  $S_{ph} = 1$ ,  $K_s = 0.1$ ,  $B = 0.0015$ ,  $\delta = 5$ ,  $\gamma = 2$ , and  $\tau_r = 10$ ): (a)  $S_r = 0$  (1), 10 (2), 12 (3), 15 (4), and 18 (5); (b)  $S_r = 18$  and  $\xi = 1.5$  (1 and 1'), 3 (2), and 4.5 (3); curve 1' shows the maximum temperature.

temperature at various points of the surface being treated (Fig. 7b) (in the case of a strong temperature dependence of the reaction rate and high heat release) can be divided into segments of inert heating and chemical transformation. The time  $\tau_i$  separating these segments and determined according to a certain criterion can be called the time of switching off of the chemical reaction or the time of the beginning of dissolution. The plateau on the temperature curves corresponds to the melting point of the base. It should be noted that in coating practice, exothermally reacting compositions are often added to the modifying powders. The model proposed here is applicable to this case, too.

Here we give the results of a parametric study of only the one-dimensional model. A detailed analysis of the two-dimensional problem shows that the nature of the process does not change; moreover, the changes of the critical parameters and the quasisteady-state characteristics of the surfacing process are insignificant. An analysis of the two-dimensional model yields additional information concerning the size of the molten pool and the zones of thermal influence.

In conclusion, we make some remarks. The real powders used to modify the surface properties of materials have a complex composition and contain both soluble and insoluble particles; dissolution yields both solid solutions and chemical compounds in the form of separate inclusions; the chemical reactions accompanying the dissolution include both endothermic and exothermic stages. A mathematical model appropriate for the analysis of the real systems should take into account the features of all models used to analyze individual systems [6–10]. We are not



aware of experimental results on the influence of process parameters on the phase and chemical compositions of coatings for soluble powders. However, in [4, 5] it is noted that the fraction of the soluble part of the powders decreases with increasing density of the electron beam power. This confirms the possibility of using the proposed model to analyze the real processes considered.

The effective source of heat in the heat-conductivity equation due to the electron-beam action can be considered a surface source since the electron penetration depth is much smaller than the thickness of the heated layer  $x_T$  formed in the material being treated for a certain characteristic time  $t_*$ . This quantity — the time of residence of the electron beam at each given point — can be estimated by the relation  $t_* = a_t/v$ . Then,  $x_T = \sqrt{a_t \lambda / (c \rho v)}$ . Assuming that  $a_t = 0.5$  cm,  $v = 1$  cm/sec,  $\lambda = 2.2$  J/(cm·sec·K),  $c = 1.086$  J/(g·K),  $\rho = 2.87$  g/cm<sup>3</sup>, we obtain  $x_T \approx 0.61$  cm. For higher thermal conductivity, the value of  $x_T$  is naturally higher. Hence, it can be assumed that in time  $t_*$ , details that have the shape of a thin plate (for example, sheet steel, flat knives, etc.) are heated over thickness almost uniformly. This allows the model proposed to be used to describe real experiments. The model is directly applicable to the description of the thermal treatment of metal foils on a heat-insulating support. If the thickness of a part far exceeds the specified value, corrections are required. Thus, the heat-conductivity equation does not contain a term that takes into account heat exchange with the ambient medium under the Newton law. It should be noted that in experiments [1–3], convective heat losses are negligible compared to the heat losses due to the radiation considered in the model. This term, however, can describe heat losses from the molten pool into the bulk of the material or into the support. This is sufficient to study the processes occurring in the molten pool, including dissolution processes. Another method of accounting for these losses consists of changing the values of the effective (equivalent) heat flux, which is used, as a rule, in modeling welding, cutting, surfacing, and laser and electron-beam processing.

## REFERENCES

1. A. A. Shipko, I. L. Pobol, and I. G. Urban, *Hardening of Steels and Alloys by Electron-Beam Heating* [in Russian], Nauka i Tekhnika, Minsk (1995).
2. S. I. Belyuk and V. E. Panin, “Electron-beam powder metallurgy in vacuum: Equipment, technology, and application,” *Fiz. Mezomekh.*, **5**, No. 1, 99–104 (2002).
3. S. I. Belyuk, V. G. Durakov, I. V. Osipov, and N. G. Rempe, “Electron-beam complex for surfacing and its application in industry,” in: *Proc. of the VIth Int. Conf. on Modifying Material Properties by Particle Beams and Plasma Flows* (Tomsk, September 23–28, 2002), Izd. Dom Kursiv, Tomsk (2002), pp. 75–78.
4. N. K. Gal’chenko, A. V. Shilenko, V. P. Samartsev, et al., “Structure formation in the Ti–B–Fe system subjected to an electron beam,” *ibid.*, pp. 307–310.
5. N. K. Gal’chenko, B. V. Dampilon, and S. I. Belyuk, “Formation of the structure and properties of ceramic-metal coatings based on titanium carbonitrides,” *Fiz. Mezomekh.*, **7**, Special issue, Part 2, 181–184 (2004).
6. O. N. Kryukova and A. G. Knyazeva, “Effect of the dynamics of particle supply to a melt on the phase structure and properties of coatings produced by electron-beam surfacing,” *ibid.*, pp. 205–208.
7. O. N. Kryukova and A. G. Knyazeva, “Modeling the structure and composition of a coating produced by electron-beam surfacing,” *Fiz. Mezomekh.*, **7**, No. 2, 81–89 (2004).
8. O. N. Kryukova, A. G. Knyazeva, and R. A. Bakeev, “Numerical study of the modes of formation of the coating structure during electron beam surfacing,” in: *Proc. of the 12th Int. Conf. on Radiat. Phys. and Chem. of Inorganic Materials* (Tomsk, September 23–27, 2003), Politech. Univ., Tomsk (2003), pp. 300–305.
9. O. N. Kryukova and A. G. Knyazeva, “Influence of the intake rate of particles into the melt on the structure and properties of coating forming during electron-beam surfacing,” in: *Proc. of the 7th Int. Conf. on Modificat. of Materials with Particle Beams and Plasma Flows* (Tomsk, July 25–30, 2004), Inst. Optic. Atmosphere, Tomsk (2004), pp. 183–186.
10. A. G. Knyazeva, O. N. Kryukova, and N. V. Bukrina, “Numerical modeling of the coating property formation during electron-beam surfacing,” in: *Abstr. 2nd Conf. of the Asian Consortium for Comput. Materials Sci.* (Novosibirsk, July 14–16, 2004), Inst. of Inorganic Chem., Sib. Div., Russian Acad. of Sci., Novosibirsk (2004), p. 111.
11. E. M. Vigdorichik and A. B. Sheinin, *Mathematical Modeling of Continuous Dissolution Processes* [in Russian], Khimiya (Leningrad Otd.), Leningrad (1971).

12. G. A. Aksel'rud and A. D. Molchanov, *Dissolution of Solid Substances* [in Russian], Khimiya, Moscow (1977).
13. O. N. Kryukova and A. G. Knyazeva, "Crystallization of a moving molten pool with a disperse phase being dissolved," in: *Abstracts of the All-Russian Conf. on Theory and Applications of Free-Boundary Problems* (Biisk, July 2–6, 2002), Inst. of Hydrodynamics, Sib. Div., Russian Academy of Science, Novosibirsk (2002), pp. 53–54.
14. O. N. Kryukova and A. G. Knyazeva, "Crystallization of a moving molten pool with a soluble disperse phase", in: *Abstracts of the All-Russian Conf. on Fundamental and Applied Problems of Modern Mechanics* (October 2–4, 2002), Izd. Tomsk. Gos. Univ. (2002), pp. 80–81.
15. N. N. Rykalin, I. V. Zuev, and A. A. Uglov, *Foundations of Electron Beam Processing of Materials* [in Russian], Mashinostroenie, Moscow (1978).
16. A. N. Tikhonov and A. A. Samarskii, *Equations of Mathematical Physics* [in Russian], Nauka, Moscow (1972).
17. I. S. Grigor'ev and E. Z. Meilikhov (eds.), *Physical Quantities* [in Russian], Énergoatomizdat, Moscow (1991).
18. N. N. Stolovich and N. S. Minit'skaya, *Temperature Dependences of the Thermal-Physical Properties of Some Metals* [in Russian], Nauka i Tekhnika, Minsk (1975).